Inorganic Chemistry Research

Article

Ab-initio Study of Bulk, Slab and Super Cell of Cesium Halide Perovskite

Ali Hossein Mohammad Zaheri[a,*], Hadi Mohammad Zaheri[b]

[a]Department of Physics, Faculty of Science, Payame Noor University, Tehran, Iran
[b]Department of Computer, Faculty of Engineering, Islamic Azad university of Arak, Arak, Iran

Received: January 30, 2024; Accepted: February 15, 2024
Cite This: *Inorg. Chem. Res.* **2023**, *7*, 51-58. DOI: 10.22036/j10.22036.2024.440809.1158

Abstract: With the remarkable progress seen in perovskite solar cell technology over the past few years, scientists have dedicated significant efforts to exploring the unique characteristics of perovskite halide materials like CsPbI3. This particular perovskite exhibits a comparatively higher stability when compared to other inorganic alkaline cations. In other words, given the rapid development of perovskite solar cells in recent years, researchers have paid special attention to studying the properties of perovskite halide materials such as $CsPbI_3$. This perovskite is relatively more stable than other inorganic alkaline cations. For this reason, this work is dedicated to the study of the electronic structure of $CsPbI_3$ in bulk, super cell and slab modes of this material. For this purpose, the quantum espresso package, which is based on density functional theory, was used. In the first step, a variable cell stability algorithm was implemented to achieve the lowest total energy value and to obtain the optimal grid parameters in bulk mode. Also, the ultra-soft quasi-potentials and *pbe* correlation performance of the quantum espresso site were used as the input file data wherever needed. To examine the surface properties of this perovskite, a three-layer slab with Miller 001 indices was designed and fabricated. In other words, the (001) surface of the emerging photovoltaic material cesium lead triiodide ($CsPbI_3$) is studied. Also, a super cell with dimensions of 2 * 2 * 2 was made and its electronic structure was studied. We found that our results are consistent with those of other works whatever available.

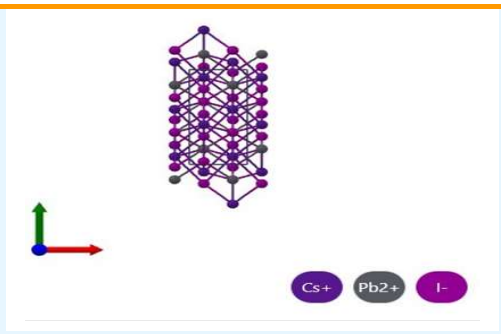

Keywords: Perovskite halide, Quantum Espresso package, Solar cell of $CsPbI_3$,$CsPbI_3$ electronic structure, Slab and super cell of $CsPbI_3$

1. INTRODUCTION

Perovskite include a wide range of materials comprising many compounds, whereas even within a chemical formula many components can be combined.[1-2] This material was named after the Russian mineralogist Lev Perovskite who was the first to describe the compositional properties of $CaTiO_3$.[3] Many perovskite have the chemical formula ABX_3, where A and B are monovalent and divalent cations, respectively, and X is a halogen atom. Due to the presence of halogen atoms, these materials are known as perovskite halides.[4] An organic or inorganic molecule can replace cation A; for example, methyl ammonium, formaldehyde, etc., which are called compound perovskite halides.[2,4-6] In recent years, perovskite solar cells (PSCs) have generated the increased attention within the photovoltaic community. The most common PSC photo absorbers are hybrid organic-inorganic halide perovskite (HPs) with an ABX_3 structure. The most common perovskite solar cells (PSC), which is known also photo absorbers are hybrid organic-inorganic halide perovskite. (HPs) with an ABX3 structure.HPs are the most promising materials for next-generation photovoltaic technologies, as reflected by their rapidly rising power conversion efficiency (PCE), reaching ~25%.[7-8] One of the inorganic compounds having attracted the point of researchers due to its electronic structure and physical properties which are proportional for solar cells is the $CsPbI_3$.

Due to its unique properties such as efficient photovoltaic cells, thermoelectric materials, stability and band gap engineering and the like, it also has potential applications such as solar cells, light emitting diodes, thermoelectric devices, photo detectors, sensors and catalysts. We have motivated to study this perovskite halide. Their outstanding properties for optoelectronic applications include optimal band gaps, excellent absorption in the visible range of the solar spectrum, exceptional transport properties for both electrons and holes, flexibility of composition engineering, and low cost in both materials and fabrication.[9-11] Therefore, we were motivated to expand our work to investigate the electronic structure of this material in the bulk, slab and super cell states of this perovskite.

It is noteworthy that mineral perovskite, despite having thermal stability in compounds, but iodine-rich compounds (iodide) are structurally unstable. Therefore, there is a major problem for research on experimental

methods in iodine-rich inorganic lead halide perovskite. In other words, the difficulty of studying experimental techniques of structural change in environmental conditions from black perovskite to non-yellow perovskite is undesirable.[1,12-14] To find the underlying cause of structural instability of the $CsPbI_3$, an accurate and deep understanding of this polymorph is required. Some different reports are available for the structure of this perovskite i.e., "mono clinically distorted perovskite structure", tetragonal and orthorhombic structures.[15-16] The undesirable phase transition of $CsPbI_3$ is due to the very small size of the Cs cation for supporting the PbI6 in the cubic perovskite structure.[17,18] With Cs substituted with larger cations such as MA or FA, the undesirable phase transition can be controlled.[19-21] But with this change, the amount of the band gap increases, so their use will not be suitable for optoelectronic devices. On the other hand, by adding a proportional quantity of hydro iodic acid under standard atmospheric conditions, the stabilization of alpha-$CsPbI_3$ can be increased. However, this method can be done with a sequential process of isopropanol.[14,15] The results of research have shown that this material is suitable for use in selected photovoltaic and optical devices.[22-25] Also, various studies on this material have increased its power conversion efficiency from 3 to22.6%.[24,26-28]

The following sections of the article are organized as follows. In the second part, we present the calculation method, which is a simulation method. The third section is devoted to results and discussion. The fourth section, which is the final section, summarizes the results and discussion.

Because of so useful and unique properties of halide perovskite the researchers are motivated to investigate these materials by ab-initio study methods.[29-32]

2. COMPUTATIONAL METHOD

By calculating the energy bands of materials, the physical properties of materials can be understood. We first investigated the electronic structure of the $CsPbI_3$ compound in the bulk state. From the different phases of this combination, the simple cubic phase have been chosen. We also used the GGA approximation to perform the calculations. Using the calculation results, we have plotted the structure of the energy bands of this compound along with different symmetric lines (Figure 1a). In this graph, the energy scale is expressed in electron volt and the source of energy is at the maximum valence band. This figure shows a direct band gap with the amount of 1.3 (E_g = 1.3 eV) and at the gamma point. The zero point of the energy axis indicates the highest occupancy in the Fermi level.

To study electronic structure, we have to investigate the behavior of the electrons of the valence and conduction bands of the materials. For this aim, one of the methods which have most frequently been used by the researchers is the self-consistent solution of the Kohn-Sham equations[33-34] which are based on density-functional theory (DFT). The simulation method which has been used in this work is the so-called QUANTUM ESPPRESSO (acronym for open-Source computer codes for electronic-structure calculations and materials modeling at the nanoscale). This package is a set of computer codes to calculate electronic-structure and materials simulation based on density- functional theory (*DFT*), pseudo potentials and plane waves (*PW*). In other words it is an integrated suite of open-source computer codes for electronic-structure calculations and materials modeling based on quantum mechanics. It is primarily designed for simulating the properties of materials at the atomic and electronic levels.

One of the important quantities for using this package is pseudo potential. Pseudopotentials are approximations that reduce the computational time by replacing the core electrons with a simplified potential. These quantities are constructed to represent the combined effect of the core and valence electrons. They are designed to reproduce the same valence electron wave functions and eigenvalues as the full electron-electron interaction while simplifying the treatment of core electrons. Of course there are a few models of pseudopotentials which we have used ultrasoft pseudo potential (uspp/usp) among from them for.

Also, we have used PbEsol (Perdew-Burke-Ernzer for solids) as the exchange correlation functional which belongs to the generalized gradient approximations (*GGA*) classes. It is worth to notice that this functional approximation is successful in calculating the structural properties but fails to reproduce the exact energy gap in semiconductor the same as perovskite. Of course, it also gives the shape of the bands correctly. Since the other approximations have the same problem with a slight difference,[35-37] it is recommended that to obtain the band gap energy we should use the results of the experimental works which have been done by other researchers.

In this work, we have done structural optimization to ground state namely "relaxation run", to clarify charge density (*dos* run), and its projection onto electronic orbitals (pdos run) and obtain energy level along a path of wave vector (*bands* run). In other words, we have studied the electronic structure, density of states, and also the role of each atom on the physical properties of this perovskite ($CsPbI_3$) structure by using density functional theory for the bulk, slab and super cell states. There is an important task for which we have to choose a set of k-points as a k-path in the step of the band run.

For this purpose, first, we have obtained the best Monkhorst-Pack grid in the first Brillion zone[38] which we have done in the step of determining the equilibrium lattice constant and the result is 8*8*8. Of course, in the next steps, we have used a denser grid (10*10*10) to

perform more accurate calculations. In the step of the band run, the Brillion zone was sampled using a set of paths based on symmetry axes, Gamma centered k-point mesh. The utilized plane wave kinetic energy cut-off, a charge density
cut-off, and the scf convergence criterion, used as the data of the input file, are considered to be 40, 240, and 10 Nano Ry, respectively.

3. RESULTS AND DISCUSSION

The optimization of the lattice constant is relaxed to 12.1209779969 angstroms. As mentioned in the previous section, to obtain this lattice constant, we changed it until the smallest total energy value was obtained. By calculating the electronic band structure, we investigated the electron wave function at each wave number (k). In the other words, the electronic band structure is the curve of the energy versus the k-wave field, which shows the allowed energy range as well as those that do not allow wave action. The valence band is a band filled with electrons. In Figure 1, the valence band is below the Fermi energy (Ef), while the conduction band is above the Fermi energy.

In facts, by calculating the structure of the electron band, the electron wave function was obtained for all wave numbers (k) and for the bulk, slab and 2 * 2 * 2 super cell modes. The band gap shows the amount of energy for moving an electron from valence band to conduction band. Therefore, low-energy band gap materials are suitable for optoelectronic devices. There are two different direct and indirect band gaps for semiconductors. If the minimum band conduction and a maximum of valence band have the same k-point value, the band gap is known as a direct band gap; otherwise, it is an indirect band gap. In order to facilitate the comparison of the electronic structure ofbulk, slabs and super cell cells states, the results of the study of these structures are presented in Figures 1a to 1c, respectively. As can be seen in these figures, the band gap is a direct type for all three modes, but its amount for the slab is greater than that for the super cell, and the amount of the super cell band is greater than that of bulk mode.

According to the definition of n-type and p-type semiconductors, which states, in n-type semiconductors, the energy level is close to the conduction band and far from the valence band. While in the p-type semiconductor, the energy level of the acceptor is close to the valence band and far from the conduction band. As seen in Figure 1a (in the bulk state), $CsPbI_3$ is known to be, a p-type semiconductor. This is more clear in slab (Figure 1b) and super cell (Figure 1c) mode.

In this work, according to the results of the density of states, the energy band gap of the perovskite $CsPbI_3$ is obtained to be 1.3 (eV) for bulk state. By comparing the graphs of band structure and density of state, it can be

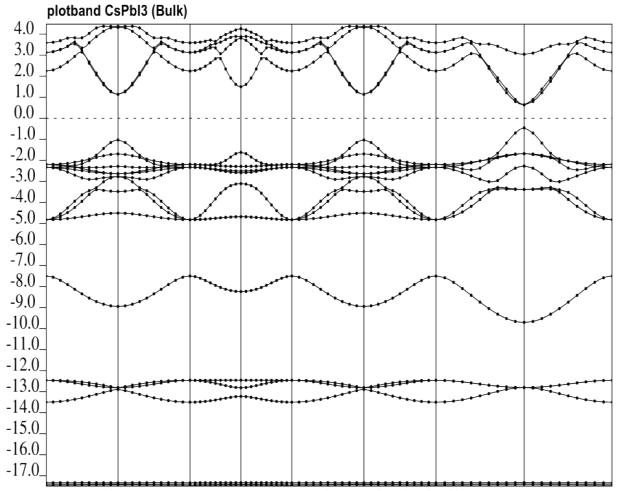

Figure 1a. Electronic structure of $CsPbI_3$ in bulk (bulk) state.

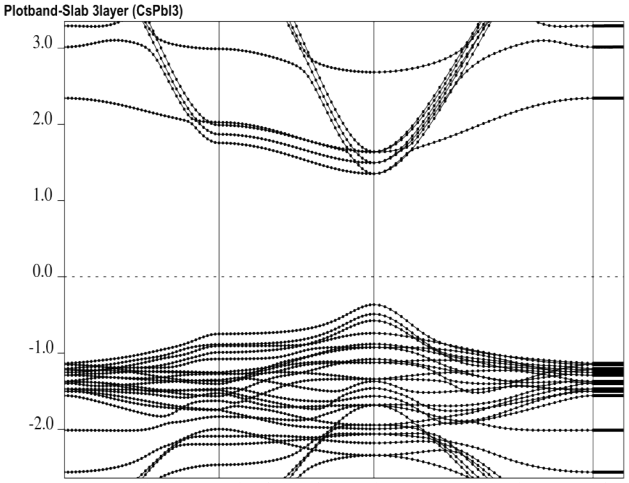

Figure 1b. Diagram of the electronic structure of a $CsPbI_3$ semiconductor in the slab state.

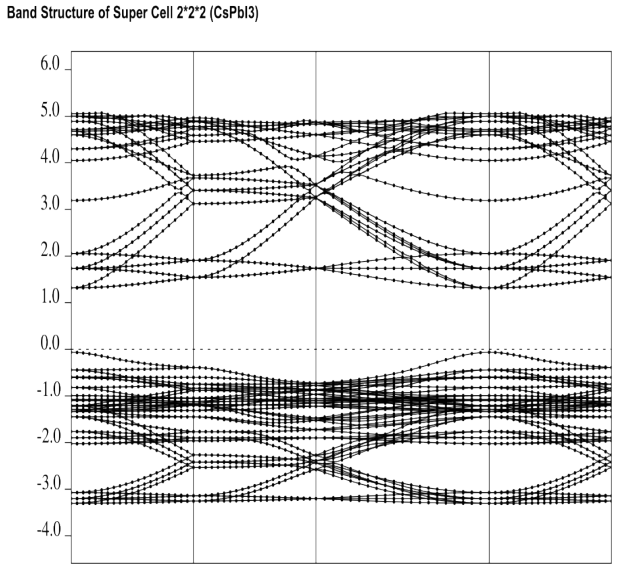

Figure 1c. Diagram of the electronic structure of $CsPbI_3$ semiconductor in 2 * 2 * 2 supercellmode.

seen that this value is in good agreement with the results of the band structure.

The role of electrons in different orbitals can be investigated by plotting the partial density of state diagrams. To investigate the role of iodine atom in this perovskite, the partial density of state diagrams for the S and P orbitals of iodine atom in bulk, slab, and super cell states was studied and the results are shown in Figures 2a to 2c, respectively. As can be seen in these figures, for the bulk state near the Fermi surface, the S and P orbitals are most likely to be occupied. But for the slab mode, this probability is slightly lower than the Fermi level, and in the super cell mode, it is almost similar to the bulk mode. The role of the various orbitals of the cesium, lead, and iodine atoms is shown in Figure 3a to 3c, respectively.

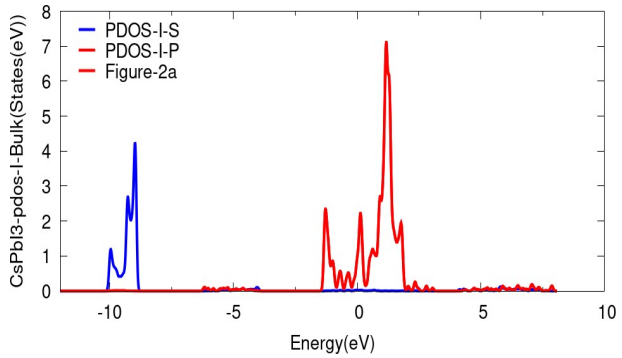

Figure 2a. Partial density of states of I in bulk mode.

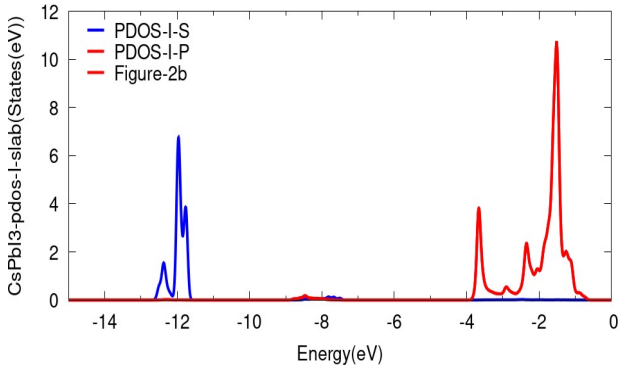

Figure 2b. Partial density of states of I in slab state (2b).

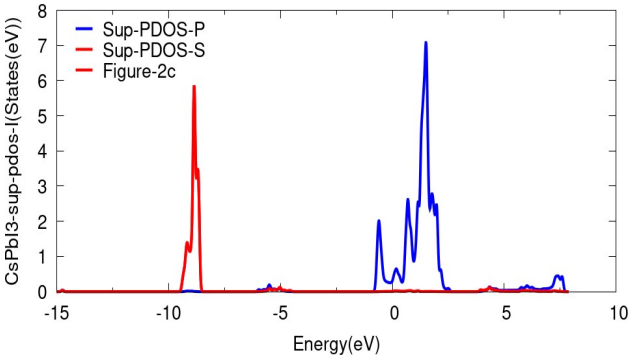

Figure 2C. Partial density of states of I in 2 * 2 * 2 supercell mode (2c).

In other words, Figure 3a to 3c show the density diagrams of the states for the S and P orbitals of the cesium atom in the bulk, slab, and super cell states. As can be seen in these graphs, for the bulk state near the Fermi surface, the S and P orbitals are most likely to be occupied. But for the slab mode, this probability is slightly lower than the Fermi level, and in the super cell mode, it is almost similar to the bulk mode. Therefore, it can be said that iodine and cesium atoms have a similar structure in this perovskite.

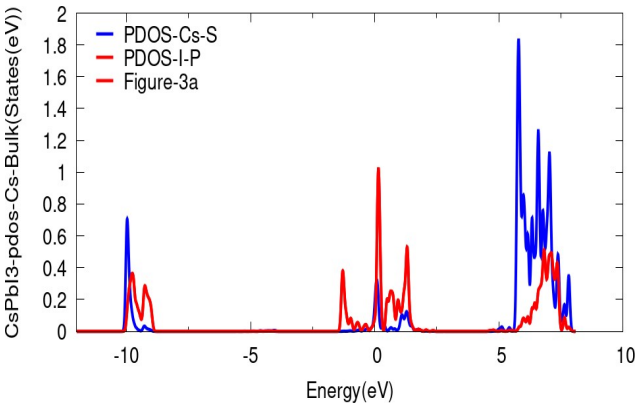

Figure 3a. Partial density of states of Cs in bulk mode.

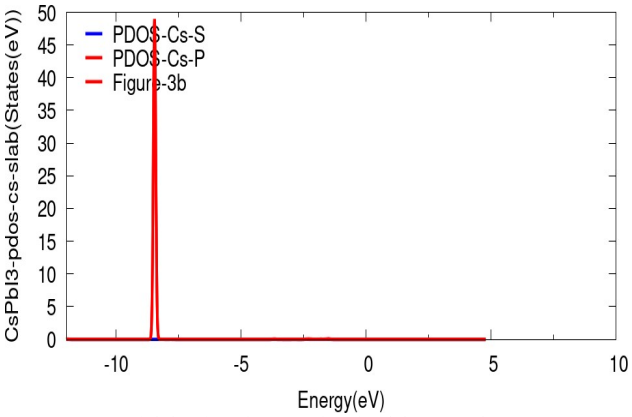

Figure 3b. Partial density of states of Cs in slab state (3b).

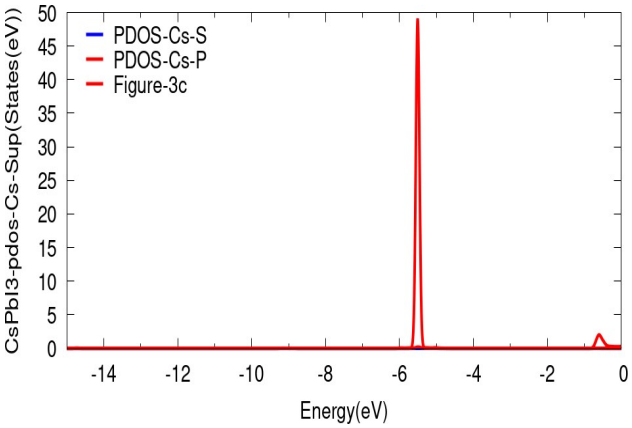

Figure 3c. Partial density of states of Cs in 2 * 2 * 2 supercell mode (3c).

For a more detailed study of the role of different atoms in the valence and conduction bands, the partial density of states for all three atoms of this semiconductor was studied. The results are shown in the following diagrams. The diagram for the lead atom is shown in Figures 4a to 4c. These graphs are similar to those of groups 2 and 3, but for thelead atom. The diagrams show that for the bulk and super cell mode, the probability of occupying the S and P orbitals near the Fermi surface is higher than that of other electronic circuits of the lead atom, while the value for the slab is lower than that of the Fermi level. As observed from Figures 4a to 4c, the electrons which occupied 2p and 2s orbitals of Cesium have the highest and the lowest occupancy of the valence band, respectively. Bycomparing the diagrams of groups 2 to 4, also it can easily be observed that the density contribution of the cesium atoms in the valence band is several times greater than that ofthe lead and iodine atoms.

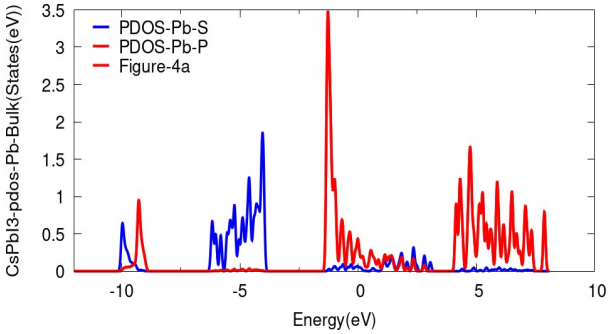

Figure 4a. Partial density of states of Pb in bulk mode.

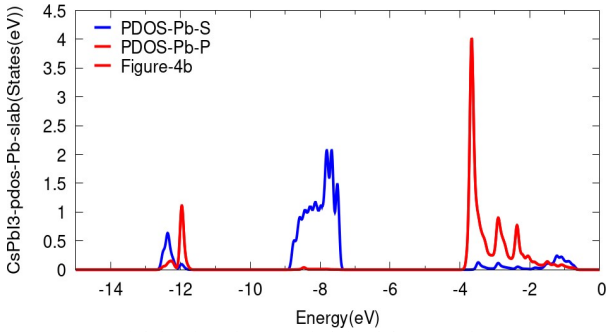

Figure 4b. Partial density of states of Pb in slab state (4b).

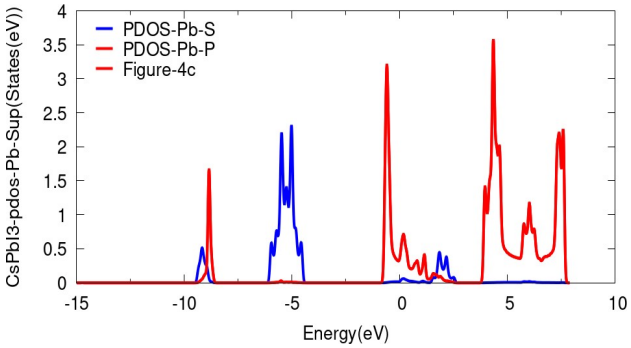

Figure 4c. Partial density of states of Pb in 2 * 2 * 2 supercell mode (4c).

In order to investigate the electron density in filling the orbitals of this semiconductor inbulk, slab and super cell states, the DOS part of the quantum espresso package was run, the obtained results of which are shown in Figures 5a to 5c. As can be seen in the figures,the peaks corresponding to the bulk and super cell states are similar to each other and areround the Fermi surface, while for the slab state they are lower than the Fermi surface. Also, in order to study the role of electron density in the amount of total angularmomentum related to the orbitals of this semiconductor, the PDOS section of the espresso quantum package was run for all three modes of the semiconductor as, bulk,slab and super cell. The obtained results are shown in Figures 6a to 6c. As can be seen in these figures, the peaks corresponding to the bulk and super cell states are similar to each other and around the Fermi surface, while for the slab state they are lower than the Fermi surface.

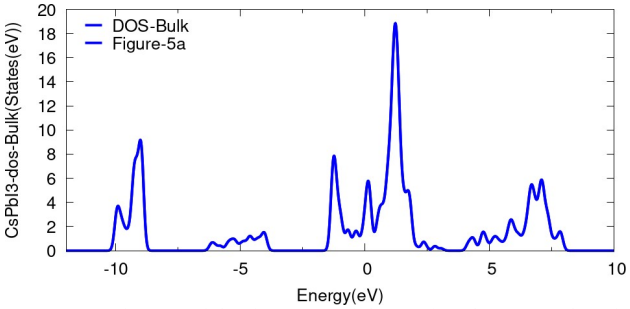

Figure 5a. Diagram of density states of the semiconductor ($CsPbI_3$) in bulk state.

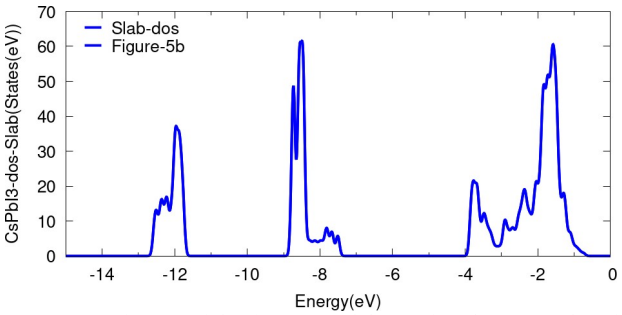

Figure 5b. Diagram of density states of the semiconductor ($CsPbI_3$) in slab state.

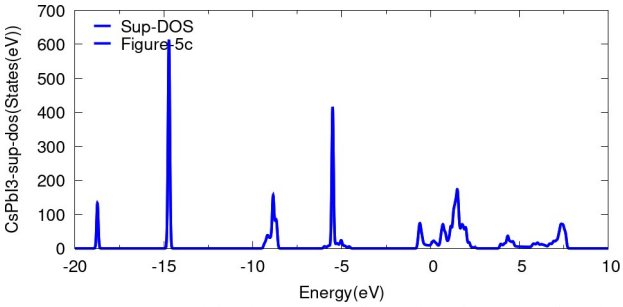

Figure 5C. Diagram of density states of the semiconductor ($CsPbI_3$) in 2 * 2 * 2 supercell state.

The results are similar to Figure 5, and these results are completely consistent with the general characteristics of this semiconductor. In the Figures (6a to 6c), it is observed that in lead atoms there is a possibility of presence of electrons of S and D orbitals in the valence band and P orbitals in the conduction band. It is also observed that around the Fermi level, there are a few peaks indicating the presence of electrons, which shows the absence of a band gap, and due to the fact that lead atom is a metal. In fact, it expresses that this research is done correctly.By comparing the fourth to sixth diagrams, it can be easily seen that the density share ofcesium atoms in the valence band is several times higher than that of lead and iodine atoms.

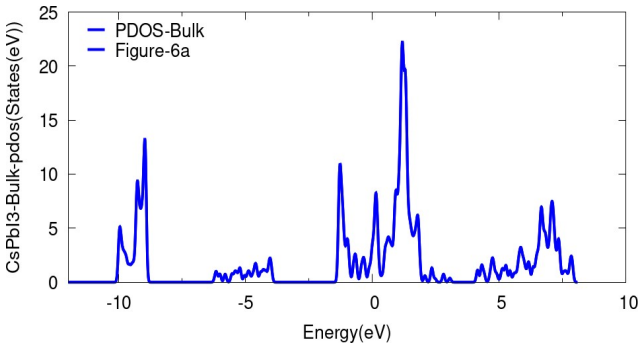

Figure 6a. Diagram of partial density states of the semiconductor ($CsPbI_3$) in bulkstate.

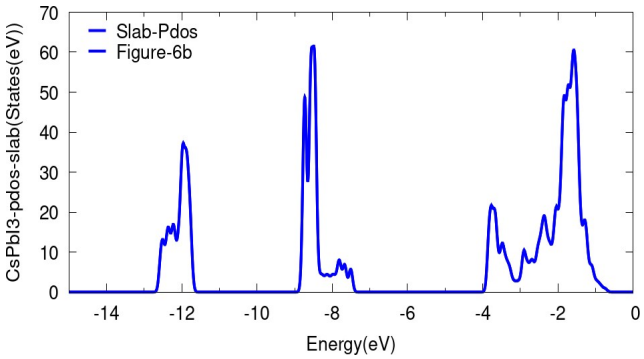

Figure 6b. Diagram of partial density states of the semiconductor ($CsPbI_3$) slab state.

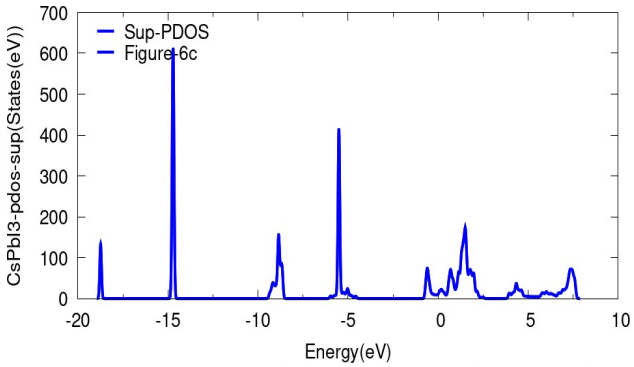

Figure 6c. Diagram of partial density states of the semiconductor ($CsPbI_3$) in 2 * 2 * 2 supercell states.

Investigation of the electronic structure of $CsPbI_3$ three-layer slabs

Due to the importance and application of Nano scale surfaces (thin films) in this section, the electronic structure of the $CsPbI_3$ slab with Miller 001 index was studied. The results of this study are shown in Figure (1b). As can be seen in this figure, there is a band gap of direct type with a value of 3 electron volts (Eg = 3 eV) at the gamma point. This study shows that the width band gap of this semiconductor in slab mode is more than that in bulk mode. This diagram contains information such as the nature of the crystal in terms of metal or non-metal, the amount of band gap energy and its type as a direct or indirect shape, as well as the distribution of electronic states in different energies.

Also, the density of states, which indicates the possibility of the presence of electrons in different orbitals, is shown in Figure (5b) for the slab state. As can be seen in this figure, there is no peak around the Fermi level, indicating that $CsPbI_3$ is semiconductor even in its slab state. To determine the role of each element for this material to be a semiconductor in slab mode, its partial density of state diagram is shown in Figure 6b.

Study of the electronic structure of $CsPbI_3$ 2 * 2 * 2 super cell.

Due to the fact that semiconductors are used in most optoelectronic devices, in thiswork, a 2 * 2 * 2 super cell of this semiconductor was designed. The electronic structure and density of states were studied. The results obtained are shown in Figure 1c. Also, the density state and partial density of states for the constituent atoms of this semiconductor were investigated, separately. The results of density state, partial density states, partial states of iodine, cesium and lead atoms are shown in Figures 2c, 3c, 4c, 5c and 6c.

Our results regarding to the bulk state are in good agreement with the results works of A. Bouhmouch *et al.* and H. R. Shanaz et al.[39-40]. Of course there is fifteen percent different between these results. This is because of kinds of approximation and potentials same as Hubbard potential and so on which they have used. But according to my best knowledge threre is no data and results for the slab and super cell states to compare with results of this work.

4. CONCLUSIONS

We have carried out the *pwscf* (plane wave self-consistent field) after the relaxation of the variable cell changing the position of atoms to minimize the total energy. After that, we have performed the band structure, dos and *pdos* runs for two-dimensional (2D) slab in direct of 001 Miller index of $CsPbI_3$ perovskite step by step.

The Density of States (DOS) graph represents the distribution of electronic states with respect to their

energy levels in a material. It essentially provides information on the number of electron states per unit energy interval at each energy level. The DOS graph is typically plotted as a function of energy on the x-axis and the density of states on the y-axis.

The Projected Density of States (PDOS) graph provides a more detailed breakdown of the DOS by attribuing the contribution of each atomic orbital or a specific group of orbitals to the total DOS. It shows how the electronic states are distributed among different atomic orbitals or groups of orbitals in the material.

Density of States (DOS) and Projected Density of States (PDOS) are both important concepts in computational materials science and condensed matter physics. They provide insights into the electronic structure of materials, but they represent different aspects of that structure.

In order to obtain the band structure and optimal lattice parameters of $CsPbI_3$, we have used the Quantum Espresso plane wave software. The utilized plane wave kinetic energy cut-off, a charge density cut-off and the scf convergence criterion are consideredto be 40, 240 and 10 Nano Ry, respectively.

As can see from the graphs of band structures, dos and pdos they have very good agreement with each other. Because near the femi level and other regions all the graphs have the same results which are explained in the above sections.

CONFLICTS OF INTEREST

The authors declare that they have no conflicts of interest.

AUTHOR INFORMATION

Corresponding Author

Ali Hossein Mohammad Zaheri: Email: ahmzaheri@gmail.com. *ORCID*: 0000-0003-1565-1677

Author

Hadi Mohammad Zaheri

REFERENCES

1. Q. Chen, N. DeMarco, Y. Yang, T. Song, C. Chen, H. Zhao, Z. Hong, *Nono Today* **2015**, *10*, 355.
2. M. Gratzel, *Nat. Mater.* **2014**, *13*, 838.
3. M. A. Pena, J. L. G. Fierro, *Chem. Rev.* **2001**, *101*, 1981.
4. S. F. Hoefler, G. Trimmel, T. Rath, *Monatsh R. Soc. Chem.* **201**, *148*, 795.
5. L. Yang, A. T. Barrows, D. G. Lidzey, T. Wang, *Rep. Prog. Phys.* **2016**, 79, 026501.
6. G. C. Papavasillou, G. Pagona, N. Karousis *J. Mater. Chem.* **2012**, *22*, 8271.
7. A. Seidu, M. Dvorak, P. Rinke, *et al. J. Chem. Phys.* **2021**, *154*, 074712.
8. National Renewable Energy Laboratory: Best research-cell efficiencies, https://www.nrel.gov/pv/assets/pdfs/best-research-cell-efficiencies.20200311.pdf, **2020.**
9. J. Troughton, K. Hooper, T. M. Watson, *Nano Energy*, **2017**, *39*, 60.
10. J. Huang, S. Tan, P. D. Lund, H. Zhou, *Energy Environ. Sci.* **2017**, *10*, 2284.
11. A. Ciccioli, A. Latini, *J. Phys. Chem. Lett.* **2018**, *9*, 3756.
12. R. J. SUtton, G. E. Eperon, L. Miranda, E. Parrott, *Adv. Energy Mater.* **2016**, *6*, 1502458.
13. Z. Yang, A. Surrente, K. Galkowski, A. Miyata, *Acs Energy Lett.* **2017**, *2*, 1621-1627.
14. G. E. Eperon, G. M. Paterno, R. J. Sutton, A. Zampetti, *J. Mater. Chem. A* **2015**, *3*, 19688-19695.
15. C. C. Stoumpos, M. G. Kanatzidis, *Acc. Chem. Res.* **2015**, *48*, 2791-2802.
16. A. Marronnier, G. Roma, S. Boyer-Richard, L. Pedesseau, *ACS Nano*, **2018**, *12*, 3477-3486.
17. B. D. Tress, W. Dar, M. I. Gao, P. Luo, *Sci. Adv.*, **2016**, *2*, 1501170.
18. L. A. Abdelhadi, M. I. Saidaminov, B. Murali, V. Adinoflfi, *J. Phys. Chem. Lett.*, **2016**, *7*, 295-301.
19. H. Choi, J. Jeong, H. B. Kim, S. Kim, B. Walter, *Nano Energy*, **2014**, *7*, 80-85.
20. Z. Li, M. Yang, J. S. Park, S. Wei, *Solid-State Alloys*. **2016**, *28*, 284-292.
21. C. Yi, J. Lou, S. Meloni, A. Boziki, *Energy Environ. Sci.* **2016**, *9*, 656-662.
22. L. M. Herz, *Annu. Rev. Phys. Chem.* **2016**, *67*, 65.
23. T. Wang, B. Daiber, J. M. Frost, S. A. Mann, E. C. Garnett, *Energy Environ. Sci.*, **2017**, *10*, 509.
24. P. Umari, E. Mosconi, F. D. Angelis, *Sci. Rep.*, **2014**, *4*, 4467.
25. J. S. Manser, J. A. Christians, P. V. Kamat, *Chem. Rev.*, **2016**, *116*.
26. C. Quarti, F. D. Angelis, D. Beljonne, *Chem. Mater.*, **2017**, *29*, 958.
27. T. C. Sum, N. Mathews, *Energy Environ. Sci.*, **2014**, *7*, 2518.
28. B. Lee, J. He, R. P. Chang, M. G. Kanatzidis, *Nature*, **2012**, *485*, 486.
29. S. Amari, S. Daoud, *Comput. Condens Matter.*, **2022**, *33*, e00764.
30. M. El Yadari, L. Bahmad, A. El Kenz, A. Benyoussef, *Phase Transit.*, **2022**, *95*, 501-514.
31. Y. Selmani, H. Labrim , S. Ziti, L. Bahmad, *Comput. Condens. Matter.*, **2022**, *32*, e00699.
32. Y. Selmani, H. Labrim, M. Mouatassime, L. Bahmad, *Mater. Sci. Semicond. Process*, **2022** *152*, 107053.
33. P. Hohenberg, W. Kohn, *Phys. Rev. B*, **1964**, *864*.
34. W. Kohn, L. J. Sham, *Phys. Rev. A*, **1965**, 1133.
35. J. Heyd, G. E. Scuseria, M. Ernzerhof, *J. Chem. Phys*. **2003**, *118*, 8207.
36. M. Paier, K. Morsman, G. Hummer, I. Kresse, *J. Chem. Phys*. **2006**, *124*, 154709.

37. C. Franchini, *J. Condens. Matter. Phys*. **2016**, *26*, 253202.
38. H. J. Monkhorst, J. D. Pack, *Phys. Rev. B*, **1976**, *13*, 135188.
39. H. R. Shanaz, B. W. Nuryadin, M. N. Subkhi, P. Pitriana, H. Aliah, *J. Phys. Conf. Ser.* **2021**, *1869*, 012206.
40. A. Bouhmouche, S. Tariq, A. Jabar, R. Moubah, H. Lassri, M. Abid, *Mater. Today: Proc., October*, **2023**.